Identification of gold nanoparticle-resistant mutants of *Saccharomyces cerevisiae* suggests a role for respiratory metabolism in mediating toxicity

Mark R. Smith[1], Matthew G. Boenzli[1], Vihangi Hindagolla[1], Jun Ding[1,2], John M. Miller[3,4], James E. Hutchison[3,4], Jeffrey A. Greenwood[2], Hagai Abeliovich[5], Alan T. Bakalinsky[1]*

Department of Food Science and Technology, Oregon State University, Corvallis, Oregon 97331-6602,[1] Department of Biochemistry and Biophysics, Oregon State University, Corvallis, OR 97331-7305,[2] The Safer Nanomaterials and Nanomanufacturing Initiative, Eugene, Oregon,[3] Department of Chemistry and the Materials Science Institute, University of Oregon, Eugene, Oregon 97403-1253,[4] Department of Biochemistry and Food Science, Hebrew University of Jerusalem, Rehovot, Israel 76100[5]

Running title: **Gold nanoparticle-resistant mutants of *S. cerevisiae***

* Corresponding author. Mailing address: Food Science and Technology, Oregon State University, Corvallis, OR 97331-6602. Phone: (541) 737-6510. Fax: (541) 737-1877. E-mail: alan.bakalinsky@oregonstate.edu.

Abstract (≤50 words)

Positively-charged gold nanoparticles (0.8 nm core diameter) reduced yeast survival, but not growth, at a concentration of 10-100 µg/ml. Among 17 resistant deletion mutants isolated in a genome-wide screen, highly significant enrichment was observed for respiration-deficient mutants lacking genes encoding proteins associated with the mitochondrion.

The increasing use of nanomaterials in industrial processes and commercial products has generated a need for systematic assessment of potential biological and environmental risks (22, 27). This task is complicated by the sheer number and variety of nanomaterials and by the multitude of assays available to assess deleterious effects. Gold nanomaterials have received significant attention because of their unique physical and chemical properties that make them well suited for both basic biological research and biomedical applications (16, 17). A number of studies have evaluated the toxicity of a variety of gold nanoparticles (reviewed in 1, 20). Although the multiplicity of both gold nanoparticle type and toxicity assay complicate direct comparisons, a number of reports indicate that the type of particle tested in the present study (~1 nm, positively-charged) can elicit toxicity (7, 13, 23, 29). While the yeast *Saccharomyces cerevisiae* has been a prominent and highly informative biological model (3), its use for evaluating the effects of nanomaterials appears to be limited based on few published reports (5, 11, 15, 18). Here, we asked whether use of the yeast model could be informative with respect to determining the toxicity of the same functionalized gold nanoparticle previously found to cause significant mortality in the embryonic zebrafish model (13).

Functionalized gold nanoparticles. Synthesis and characterization of the gold nanoparticles (AuNPs) have been described (12, 33). The particles (Au_{11}[ligand]$_{10}$) comprised a 0.8 nm 11-atom gold core, functionalized with either 1) positively-charged, N,N,N trimethylammoniumethanethiol (TMAT) as the iodide salt; 2) negatively-charged, 2-mercaptoethanesulfonate (MES) as the sodium salt; or 3) neutral 2-[2-(2-mercaptoethoxy)ethoxy]ethanol (MEEE) (Fig. 1A). Throughout this report, these functionalized gold nanoparticles are referred to as 0.8 nm AuTMAT, 0.8 nm AuMES

and 0.8 nm AuMEEE, respectively, to distinguish them from other gold nanoparticles described. Analogs of the TMAT functional group (Fig. 1B), tetramethylammonium iodide, tetramethylammonium chloride, and choline chloride, were purchased from Sigma Aldrich (http://www.sigmaaldrich.com/united-states.html).

Yeast, media, toxicity assays. *Saccharomyces cerevisiae* BY4742 (*MAT*α *his3*Δ*1 leu2*Δ*0 lys2*Δ*0 ura3*Δ*0*) was used to assess effects of the functionalized 0.8 nm AuNPs on yeast survival and growth. Strain KK86 is a *rho*^{0} derivative of BY4742 lacking mitochondrial DNA (14). A non-essential yeast gene deletion library (32) constructed in the BY4742 genetic background (YSC1054, Open Biosystems, Inc.) was screened for resistance to these gold nanoparticles. *S. cerevisiae* was grown in Yeast Nitrogen Base without amino acids (Difco) containing 2% glucose and supplemented with 20 µg/ml histidine, 30 µg/ml each of leucine and lysine, and 10 µg/ml of uracil ("YNB + supplements") to satisfy auxotrophic requirements, or in YEPD (1% yeast extract, 2% peptone, and 2% glucose).

Fluorescence microscopy. Yeast strains were grown and prepared for fluorescence microscopy essentially as described (31). Briefly, cells were grown statically for 24 h at 30°C in 200 µl of YNB in a 96-well plate, after which they were pelleted by centrifugation and fixed by resuspension in 70% ethanol at room temperature for 30 min. The fixed cells were washed once with sterile distilled water, and resuspended in 20 µl of sterile distilled water. Five µl of cell suspension were mixed with 5 µl of mounting media containing DAPI (Molecular Probes Invitrogen P36935). The mixture (2.5 µl) was spotted onto a slide, covered with a coverslip, and allowed to dry in the dark 1-2 h before sealing with transparent nail polish. Slides were held in the

dark at room temperature for up to 3 days before being visualized using a Zeiss Axiovert S100 microscope equipped with a 100x objective, 2x zoom lens, and a Photometrics CoolSNAP HQ CCD camera controlled by MetaMorph 6.3 imaging software. For visualizing DAPI, excitation and emission wavelengths were 350 and 460 nm, respectively. Autofluorescence was used to visualize cell shape; excitation and emission wavelengths were 480 and 535 nm, respectively.

Yeast growth inhibition was assessed as a reduction in cell yield (A_{600}) in treated vs control cells. Cells were grown overnight in YNB + supplements, washed twice in sterile distilled water, and then diluted 1,000-fold in duplicate 250 µl aliquots of YNB + supplements (control) or YNB + supplements + AuNPs. Cells were incubated for 48 h at 30°C and 200 RPM in 1.5 ml screw-capped polypropylene tubes in triplicate after which A_{600} values were measured.

To assess survival, cultures grown overnight in either YNB + supplements or YEPD were washed twice with sterile distilled water and then incubated in 100 µl aliquots of sterile distilled water at 10^5 to 10^7 cells/ml in 500 µl screw-capped polypropylene tubes containing each of the functionalized 0.8 nm AuNPs. At least three replicates were performed per strain at each AuNP dose. After 24 h at 30°C and 200 rpm, cells were plated on YEPD agar in duplicate and colonies were counted after 48 h at 30°C to determine survival relative to control cells incubated in parallel under identical conditions in sterile distilled water lacking AuNPs. The number of cells killed in the water-only control was subtracted from the number killed in the parallel AuNP exposures. (No differences in survival were observed between BY4742 that had been grown overnight in either YNB + supplements or YEPD.)

Screening of yeast deletion library for mutants with enhanced survival in presence of AuNPs. The non-essential yeast gene deletion library was screened for mutants that exhibited better survival than the parent strain BY4742 after 24 h incubation in sterile distilled water containing AuNPs. The library was screened in pools consisting of about 100 mutants each, suspended in sterile distilled water. To minimize the possibility of underrepresentation of slower-growing mutants, all deletion mutants were initially grown individually in 96-well plates in YEPD for 24 h at 30°C, only after which cells were pooled (1 plate per pool), washed twice in sterile distilled water, and resuspended in sterile distilled water at about 3 x 10^7 cells/ml. Pools of cells were then incubated in 100 µl aliquots of sterile distilled water at about 10^5 cells/ml in 500 µl screw-capped polypropylene tubes (1 tube per pool) containing up to 20 ppm AuNPs. After 24 h at 30°C and 200 rpm, cells were plated on YEPD agar which was incubated 48 h at 30°C. Colonies of survivors were re-streaked on YEPD and retested individually for survival after 24 h incubation in sterile distilled water in the presence of AuNPs. The survival of mutants that retested positive relative to BY4742 ($p \leq 0.05$, two-sided Student's T-test) was then evaluated at multiple concentrations of the AuNPs. The AuNP exposure protocol used to screen the library was developed based on preliminary experiments to determine conditions that the parental strain BY4742 was unable to survive.

Mutant Identification. Deletion mutants that exhibited enhanced survival were identified by sequencing mutant-specific oligonucleotide tag sequences within a PCR product generated using primers complementary to sequences shared by all mutants. Colony PCR (4) was performed using the polymerase *pfx* (Invitrogen) according to the

manufacturer's instructions. PCR products were purified (Qiaquick Spin Columns, Qiagen) following the PCR clean-up protocol, and sequenced at the Oregon State University Center for Genome Research and Biocomputing.

Assessment of toxicity. Possible deleterious interactions between the 0.8 nm AuNPs and yeast were assessed initially as the ability to inhibit growth, measured as cell yield (A_{600}) after incubation in YNB + supplements for 48 h. No reduction in yield was observed between BY4742 grown in the absence (control) and presence of the three 0.8 nm AuTMAT, AuMES, or AuMEEE at concentrations as high as 100 μg/ml (data not shown). While we are not aware of published data on the response of yeast to these 0.8nm AuNPs, a recent study reported that the same 0.8 nm AuTMAT NP and a 1.5 nm AuTMAT NP (a larger particle with the same surface coating), at concentrations ranging from 80 ppb to 250 ppm induced significantly greater lethality in embryonic zebrafish than either the negatively-charged AuMES or neutral AuMEEE NPs of the same sizes (13). A related but somewhat larger cationic AuNP (1.4 nm diameter) used to monitor endocytosis in log-phase *S. cerevisiae* spheroplasts at 5-10 μM was not reported to cause growth inhibition (10, 25, 26). (This particle is quite different than the particles used in the present study. It is coated with phosphine ligands easily displaced in biological media in the presence of thiols and has only 6 positive charges in the ligand shell compared to at least 30 positive charges in the 1.5 nm AuTMAT particle.) Because the incubation period was not longer than 90 min prior to fixation of cells for microscopic analysis, the possibility of inhibition cannot be ruled out. Nonetheless, the process of endocytosis during the incubation was not found to be abnormal. The highest 0.8 nm AuTMAT concentration tested in the present study with no apparent deleterious

139 effect on yeast growth was 21.6 μM (100 μg/ml).

140 We next tested whether the functionalized 0.8 nm AuNPs could reduce survival of
141 non-growing stationary phase cells incubated in water over 24 h. While a reduction in
142 survival was not observed for the cells incubated with the 0.8 nm AuMES or AuMEEE
143 nanoparticles, reduced survival of BY4742 was observed at 10 ppb of positively-
144 charged 0.8 nm AuTMAT, the lowest concentration tested (Fig. 2). Within the range of
145 10 ppb and 100 ppm, a linear relationship was observed between the log of the
146 AuTMAT dose and the log of the number of BY4742 cells killed. That is, a fixed number
147 of cells were killed at a given AuTMAT concentration regardless of the number of cells
148 treated, consistent with a requirement for direct and irreversible interaction between
149 cells and some minimum number of AuTMAT particles. In order to distinguish between
150 toxicity of the 0.8 nm AuTMAT nanoparticles and the positively-charged quaternary
151 ammonium functional group contained in the TMAT group alone, cells were exposed
152 independently to the TMAT analogs tetramethylammonium iodide,
153 tetramethylammonium chloride, and choline chloride (Fig. 1B) at functional group
154 concentrations ranging from 500-900 μM or 2-4 times greater on a molar basis than the
155 concentration of TMAT groups (216 μM) at the highest 0.8 nm AuTMAT dose tested,
156 100 μg/ml. No reduction in survival of BY4742 exposed to these TMAT analogs was
157 observed relative to untreated control cells incubated in parallel (data not shown).

158 **Screen of yeast deletion library for resistant mutants.** In order to determine
159 which genes might predispose yeast to 0.8 nm AuTMAT-induced damage during
160 stationary phase, mutants better able to survive the exposure were sought by screening
161 a library of non-essential yeast deletion mutants as described above, “Screening of

yeast deletion library for mutants with enhanced survival in presence of AuNPs". Initially, approximately 200 putative resistant mutants were isolated following exposure of pools of non-growing deletion mutants to a concentration of 0.8 nm AuTMAT that killed an equal number of cells of the parent strain BY4742. Upon retesting, 32 were found to be reproducibly resistant and were identified by sequence analysis of mutant-specific oligonucleotide tags. Among the 32 mutants, 17 unique gene deletions were identified from among the total 4,750 mutants screened indicating that multiple clones of the same mutants had been isolated (Table 1). As indicated in the Table 1, 12 mutants were isolated once, two were isolated twice, one was isolated four times, and two were isolated six times.

A gene ontology (GO) analysis was undertaken to correlate loss of the genes that resulted in increased cell survival with specific components, processes, and functions (Table 2). Highly significant enrichment was observed for genes whose products localize to the mitochondrion and to the mitochondrial large ribosomal subunit in particular. The process of "mitochondrial organization" and the function, "structural constituent of ribosome" were also enriched significantly. Of the seventeen genes, loss of ten has been reported to result in respiration deficiency, equivalent to a frequency of ~60%, compared to ~7% for the original library, (319 among a total of 4,750 deletion mutants; 17). This represents an approximate 9-fold enrichment ($p<10^{-4}$, chi square test). Among the 17 AuNP-resistant mutants reported here, five (*mrpl37*Δ, *ccm1*Δ, *nam2*Δ, *img1*Δ *rtc6*Δ) were found to be sensitive to hydrogen peroxide (28) and seven (*abf2*Δ, *img1*Δ, *mrpl4*Δ, *mrpl51*Δ *boi2*Δ, *stp2*Δ, *trk1*Δ) were found sensitive to either or both hydrogen peroxide and menadione (30) in previous genome-wide screens. Nine of

these mutants are missing genes encoding products associated with the mitochondrion, *mrpl37*Δ, *ccm1*Δ, *nam2*Δ, *img1*Δ, *rtc6*Δ, *abf2*Δ, *img1*Δ, *mrpl4*Δ, *mrpl51*Δ. While one study reported that a 1.4 nm gold nanoparticle coated with a negatively-charged triphenylphosphine ligand generated significant oxidative stress and mitochondrial damage in HeLa cells (23), loss of functional mitochondria in yeast has not always been reported to increase oxidative stress (7, 9).

As noted above, yeast cells were observed to take up a positively-charged triphenylphosphine-stablized 1.4 nm AuNP via endocytosis (25). Uptake was blocked in an *end3* endocytosis mutant while AuNPs accumulated in the early endosome of a *sec18* secretory mutant. No apparent signs of toxicity were noted over the short 15-90 min exposure of spheroplasts to 5 μM of these 1.4 nm gold nanoparticles. Although potential toxicity was not a specific focus of subsequent studies of endocytosis using the same positively-charged, triphenylphosphine-stabilized AuNPs and similar conditions, no reduction in cell viability was noted (10, 26). These results are consistent with our finding that yeast cell growth, assessed as cell yield, was unaffected by exposing intact cells to as much as 22 μM of the 0.8 nm AuTMAT nanoparticles, corresponding to the 100 μg/ml dose. The observation that a *trk1*Δ mutant was resistant suggests an alternative route for AuTMAT uptake. *TRK1* encodes a potassium channel and in *Candida albicans*, this same channel was found to mediate the toxicity of the cationic protein, histatin 5, whose molecular weight, 3,036 Da is close to that of the 0.8 nm AuTMAT, 4,626 Da (2). The authors proposed a model whereby binding of histatin 5 by Tkr1 distorted channel shape allowing leakage of ATP and potassium. We speculate that “jamming” of the *S. cerevisiae* Trk1 channel by the 0.8 nm AuTMAT might lead to

similar leakage of essential cytoplasmic constitutents. On the other hand, it is possible that AuTMAT could reduce cell survival in the absence of uptake through interaction with negatively-charged phosphomannans in the cell wall or phospholipids in the cell membrane.

Five of the 17 resistant mutants (*ccm*Δ, *nam2*Δ, *mrpl4*Δ, *rtc6*Δ, and *mrpl51*Δ) were reported elsewhere to excrete significant amounts of glutathione after 48 h of growth in a YNB-based medium in an independent screen of the corresponding homozygous diploids (24). Whether these mutants accumulated or excreted excess glutathione during the 0.8 nm AuTMAT exposure performed in water at 30°C over 24 h in the present study is unknown. If so, thiol exchange with glutathione may have resulted in detoxification of the original AuTMAT NP.

Dose-response of resistant mutants. Once the 17 deletion mutants were identified, dose-response analysis was undertaken on clones retrieved from the original library rather than the clones that had been exposed to the 0.8 nm AuTMAT to minimize the possibility that second-site mutations may have been selected during exposure. Table 3 lists the mutants in decreasing order of resistance to 100 ppm of 0.8 nm AuTMAT. The most resistant mutant, *mrpl51*Δ, exhibited about 6-fold better survival than the parent strain, while the least resistant mutant, YMR155wΔ, exhibited only 16% better survival. At the 10 ppm 0.8 nm AuTMAT dose, four mutants exhibited the same (*boi2*Δ, *img1*Δ, *rtc6*Δ) or worse (*abf2*Δ) survival than the parent. The other 13 mutants had better survival than the parent at both the 10 and 100 ppm 0.8 nm AuTMAT doses. One explanation for the observed enrichment in mutants impaired in mitochondrial protein synthesis is that such activity is critical for maintenance of the mitochondrial

genome (21), and that the subsequent likely loss of the mitochondrial genome in these mutants accounts for their resistance. To test this possibility, we assayed survival of KK86, a BY4742 derivative lacking mitochondrial DNA (14) following treatment with AuTMAT. At the 10 ppm dose, the survival of KK86 was found to be the same as that of BY4742, while at the 100 ppm AuTMAT dose, survival of BY4742 was 1.8 times better (p=0.032). Thus, loss of the mitochondrial genome alone does not result in resistance. All mutants were also subjected to fluorescence microscopy using DAPI to determine the presence of mitochondrial DNA with BY4742 and KK86 serving as positive and negative controls, respectively. Among the 12-27 cells scored per strain, 25-100% contained mitochondrial DNA based on observation of a single spot of prominent fluorescence with weaker spots of fluorescence throughout a cell (31) (Table S1, Fig. S1).

Was the yeast model informative with respect to assessing the potential toxicity of the 0.8 nm AuNPs tested? The observation that growing cells were insensitive to the damage observed in higher eukaryotes at similar concentrations suggests major differences in uptake or response. On the other hand, the observed susceptibility of non-growing stationary phase cells to 0.8 nm AuTMAT-mediated killing indicates similarities. Through the ability to readily link phenotype with genotype by mutational analysis, it was possible to determine that functional mitochondria appear to predispose yeast to damage. The finding that about 1/3 of the resistant mutants had previously been found to excrete significant amounts of glutathione suggests the possibility of 0.8 nm AuTMAT detoxification by thiol exchange.

We thank Alex Hadduck for technical assistance, Brian K. Kennedy for providing strain KK86, Qilin Li and Lisa Truong for helpful discussions, and anonymous reviewers for helpful criticisms. This study was funded by U.S. Environmental Protection Agency (EPA) STAR program grant R833325 to A.T.B. The Oregon State University Environmental Health Sciences Center (grant number P30 ES000210; NIEHS, NIH) provided the library of yeast deletion mutants. The Safer Nanomaterials and Nanomanufacturing Initiative provided the AuNPs through a grant from the Air Force Research Laboratory under agreement number FA8650-05-1-5041. Additional funding was provided by the W. M. Keck Foundation.

REFERENCES

1. **Alkilany AM, Murphy CJ.** 2010. Toxicity and cellular uptake of gold nanoparticles: what we have learned so far? J. Nanopart. Res. **12**: 2313-2333.

2. **Baev D, Rivetta A, Vylkova S, Sun JN, Zeng G-F, Slayman CL, Edgerton M.** 2004. The TRK1 potassium transporter is the critical effector for killing of *Candida albicans* by the cationic protein, histatin 5. J. Biol. Chem. **279**:55060-55072.

3. **Botstein D, Fink GR.** 2011. Yeast: an experimental organism for 21st century biology. Genetics **189**: 695-704.

4. **Burke D, Dawson, D, Stearns T.** 2000. Methods in Yeast Genetics. Cold Spring Harbor, Danvers, MA.

5. **Chiron JP, Lamandé, J, Moussa F, Trivin F, Céolin R.** 2000. Effect of "micronized" C_{60} fullerene on the microbial growth in vitro. Ann. Pharm. Fr. **58:**170-175.

6. **Dimmer KS, Fritz, S, Fuchs F, Messerschmitt M, Weinbach N, Neupert W, Westermann B. 2002.** Genetic basis of mitochondrial function and morphology in *Saccharomyces cerevisiae*. Mol. Biol. Cell. **13**: 847-853.

7. **Evans MV, Turton HE, Grant CM, Dawes IW.** 1998. Toxicity of linoleic acid hydroperoxide to *Saccharomyces cerevisiae*: involvement of a respiration-related process for maximal sensitivity and adaptive response. J. Bacteriol. **180**:483-490.

8. **Goodman CM, McCusker CD, Yilmaz T, Rotello VM.** 2004. Toxicity of gold nanoparticles functionalized with cationic and anionic side chains. Bioconjugate Chem. **15**:897-900.

9. **Grant CM, MacIver FH, Dawes IW.** 1997. Mitochondrial function is required for resistance to oxidative stress in the yeast *Saccharomyces cerevisiae*. FEBS Let. **410**:219-222.

10. **Griffith J, Reggiori F. 2009.** Ultrastructural analysis or nanogold-labeled endocytic compartments of yeast *Saccharomyces cerevisiae* using a cryosectioning procedure. J. Histochem. Cytochem. **57**:801-809.

11. **Hadduck AN, Hindagolla V, Contreras A, Li Q, Bakalinsky AT.** 2010. Does aqueous fullerene inhibit growth of *Saccharomyces cerevisiae* or *E. coli*? Appl. Environ. Microbiol. **76**:8239-8242.

12. **Harper SL, Carriere JL, Miller JM, Hutchison JE, Maddux BLS, Tanguay RL.** 2011. Systematic evaluation of nanomaterial toxicity: utility of standardized materials and rapid assays. ACS Nano. **5**:4688-4697.

13. **Harper S, Usenko C, Hutchison JE, Maddux BLS, Tanguay RL.** 2008. In vivo biodistribution and toxicity depends on nanomaterial composition, size, surface functionalisation and route of exposure. J. Exp. Nanosci. **3**:195-206.

14. **Kaeberlein M, Hu D, Kerr EO, Tsuchiya M, Westman EA, Dang N, Fields S, Kennedy BK.** 2005. Increased life span due to calorie restriction in respiratory-deficient yeast. Plos Genet. **1**:e69.

15. **Kasemets K, Ivask A, Dubourguier H-C, Kahru A.** 2009. Toxicity of nanoparticles of ZnO, CuO and TiO2 to yeast *Saccharomyces cerevisiae*. Toxicol. in Vitro **23**:1116-1122.

16. **Lévy R, Shaheen U, Cesbron Y, Sée V.** 2010. Gold nanoparticles delivery in mammalian live cells: a critical review. Nano Rev. **1**:4889.

17. **Ma X, Wu Y, Shubin J, Tian Y, Zhang X, Zhao Y, Yu L, Liang X-J.** 2011. Gold nanoparticles induce autophagosome accumulation through size-dependent nano uptake and lysosome impairment. ACS Nano. **5**:8629-8639.

18. **Maheshwari, V, Fomenko DE, Singh G, Saraf RF.** 2010. Ion mediated monolayer deposition of gold nanoparticles on microorganisms: discrimination by age. Langmuir **26**:371-377.

19. **Merz S, Westermann B.** 2009. Genome-wide deletion mutant analysis reveals genes required for respiratory growth, mitochondrial genome maintenance and mitochondrial protein synthesis in *Saccharomyces cerevisiae*. Genome Biol. **10**: R95.

20. **Murphy CJ, Gole AM, Stone JW, Sisco PN, Alkilany AM, Goldsmith EC, Baxter SC.** 2008. Gold nanoparticles in biology: beyond toxicity to cellular imaging. Acc. Chem. Res. **41**:1721-1730.

21. **Myers, AM, Pape, LK, Tzagoloff, A.** 1985. Mitochondrial protein synthesis is required for maintenance of intact mitochondrial genomes in *Saccharomyces cerevisiae*. EMBO J. **4**:2087-2092.

22. **Nel, A, Xia T, Madler L, Li N.** 2006. Toxic potential of materials at the nanolevel. Science. **311**:622-627.

23. **Pan Y, Leifert A, Ruau D, Neuss S, Bornemann J, Schmid G, Brandau W, Simon U, Jahnen-Dechent W.** 2009. Gold nanoparticles of diameter 1.4 nm trigger necrosis by oxidative stress and mitochondrial damage. Small **5**:2067-2076.

24. **Perrone GG, Grant CM, Dawes IW.** 2005. Genetic and environmental factors influencing glutathione homoeostasis in *Saccharomyces cerevisiae*. Mol. Biol. Cell **16**:218-230.

25. **Prescianotto-Baschong C, Riezman H.** 1998. Morphology of the yeast endocytic pathway. Molec. Biol. Cell. **9**:173-189.

26. **Prescianotto-Baschong C, Riezman H.** 2002. Ordering of compartments in the yeast endocytic pathway. Traffic **3**:37-49.

27. **Shaw SY, Westley EC, Pittet MJ, Subramanian A, Schreiber SL, Weissleder R.** 2008. Pertubational profiling of nanomaterial biologic activity. Proc. Natl. Acad. Sci. **105**:7387-7392.

28. **Thorpe GW, Fong CS, Alic N, Higgins VJ, Dawes IW.** 2004. Cells have distinct mechanisms to maintain protection against different reactive oxygen species: oxidative-stress-response genes. Proc. Natl. Acad. Sci. **101**:6564-6569.

29. **Truong L, Tilton SC, Zaikova T, Richman E, Waters KM, Hutchison JE, Tanguay RL.** 2012. Surface functionalities of gold nanoparticles impact embryonic gene expression responses. Nanotox. doi: 10.3109/17435390.2011.648225.

30. **Tucker CL, Fields S.** 2004. Quantitative genome-wide analysis of yeast deletion strain sensitivities to oxidative and chemical stress. Compar. Function. Genomics. **5**:216-224.

31. **Williamson DH, Fennell DJ.** 1975. The use of fluorescent DNA-binding agent for detecting and separating yeast mitochondrial DNA, p 335-351. *In* Prescott, DM (ed), Methods in cell biology, vol XII, yeast cells, Academic Press, NY.

32. **Winzeler EA, Shoemaker DD, Astromoff A, Liang H, Anderson K, et al.** 1999. Functional characterization of the *S. cerevisiae* genome by gene deletion and parallel analysis. Science. **285**:901-906.

33. **Woehrle GH, Hutchison JE.** 2005. Thiol-functionalized undecagold clusters by ligand exchange: synthesis, mechanism, and properties. Inorganic Chem. **44**:6149-6158.

Figure Legends

Figure 1. Structures of the 0.8 nm AuNPs and analogs. (A) Functional groups used to derivatize the nano gold particles. Positively-charged trimethylammoniomethanethiol (TMAT); negatively-charged 2-mercaptoethanesulfonate (MES); and neutral 2-[2-(2-mercaptoethoxy)ethoxy]ethanol (MEEE)**.** (B) Structures of TMAT functional analogs. The molecular weights of AuTMAT, tetramethylammonium chloride, tetramethylammonium iodide, and choline chloride are 4,625.67, 109.6, 201.05, and 139.63 Da, respectively.

Figure 2. Stationary-phase BY4742 cells killed as a function of AuTMAT concentration. Cells were grown in either YEPD or YNB, washed, and suspended in sterile distilled water alone (control), or sterile distilled water supplemented with AuTMAT at 200 rpm and 30°C. Survival was assessed by plating onto duplicate YEPD plates after a 24-h incubation. Cells killed in the water-only control were subtracted from number of cells killed in the AuTMAT exposures. Data are means of four experiments with three to sixteen replicates performed at each concentration. Error bars are standard deviations.

Figure S1. DAPI-staining of AuTMAT-resistant mutants. Upper panel, DAPI fluorescence; lower panel, autofluorescence. BY4742 and KK86 are positive and negative controls for the presence of mitochondrial DNA, respectively. Reference bar, 10 μm.

Figure 1

A.

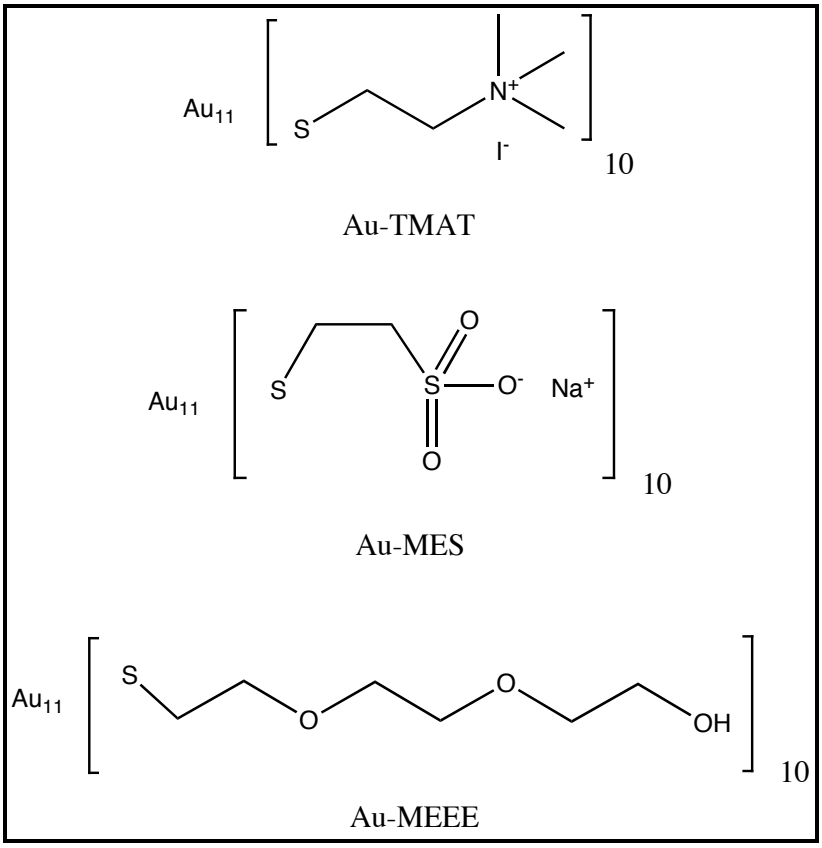
Au11
S
N+
I-
10
Au-TMAT
Au11
S
S
O
O
O-
Na+
10
Au-MES
Au11
S
O
O
OH
10
Au-MEEE

B

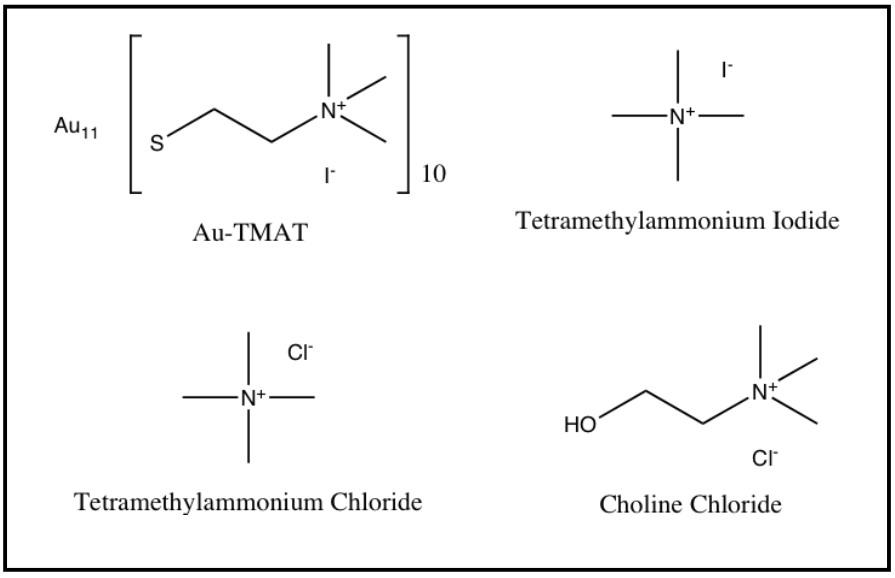
Au11
S
N+
I-
10
Au-TMAT
I-
N+
Tetramethylammonium Iodide
Cl-
N+
Tetramethylammonium Chloride
HO
N+
Cl-
Choline Chloride

Figure 2

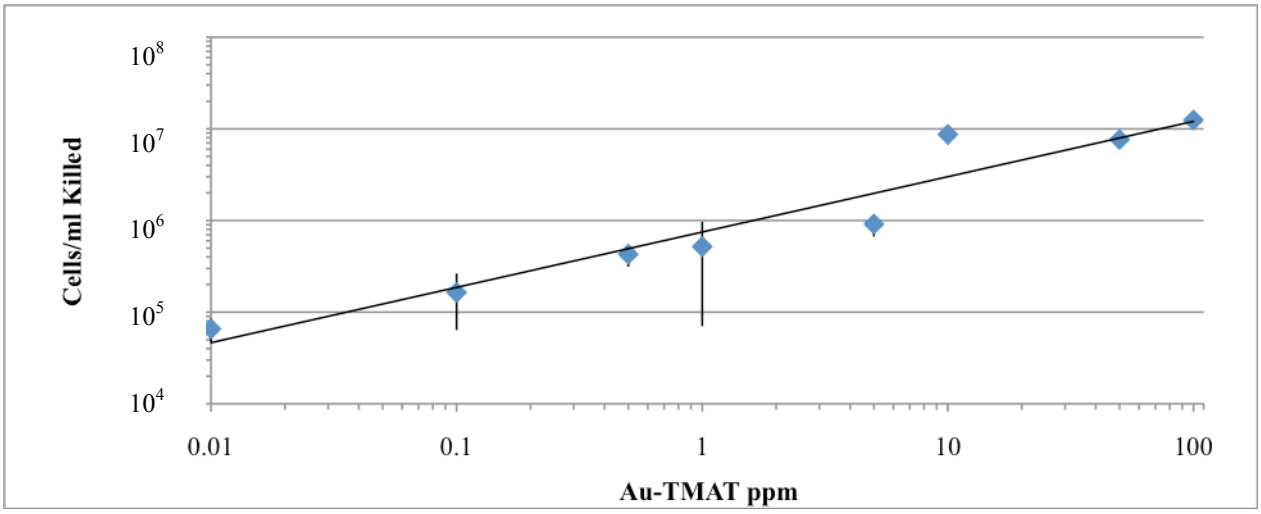

402 **Table 1.** List of genes[a] whose loss confers resistance to 0.8 nm AuTMAT.

Locus	**Gene name (number of times mutant was isolated)**	**Function** (SGD summary 25 Dec 11)	**RD**[b]
YBR268w	*MRPL37* (2)	Mitochondrial ribosomal protein of the large subunit.	yes
YCR046c	*IMG1* (1)	Mitochondrial ribosomal protein of the large subunit, required for respiration and maintenance of mitochondrial genome.	yes
YER114c	*BOI2* (1)	Protein implicated in polar growth, functionally redundant with Boi1p; interacts with bud-emergence protein Bem1p; contains an SH3 (src homology 3) domain and a PH (pleckstrin homology) domain.	yes
YGL166w	*CUP2* (1)	Cu-binding transcription factor; activates transcription of metallothionein genes CUP1-1 and CUP1-2 in response to elevated Cu concentrations.	no
YGR150c	*CCM1* (2)	Mitochondrial 15s rRNA-binding protein; required for intron removal of COB and COX1 pre-mRNAs; has pentatricopeptide repeat (PPR) motifs; mutant has defective plasma membrane electron transport.	yes
YGR207c	*CIR1* (4)	Mitochondrial protein that interacts with frataxin (Yfh1p); putative ortholog of mammalian electron transfer flavoprotein complex subunit ETF-beta;	no

		may play role in oxidative stress response.	
YHR006w	*STP2* (6)	Transcription factor, activated by proteolytic processing in response to signals from the SPS sensor system for external amino acids; activates transcription of amino acid permease genes.	yes
YJL129c	*TRK1* (1)	Component of Trk1p-Trk2p K transport system; 180 kDa high affinity K transporter; phosphorylated in vivo and interacts physically with phosphatase Ppz1p, suggesting Trk1p activity is regulated by phosphorylation.	no
YLR382c	*NAM2* (6)	Mitochondrial leucyl-tRNA synthetase, also has direct role in splicing of several mitochondrial group I introns; indirectly required for mitochondrial genome maintenance.	yes
YLR439w	*MRPL4* (1)	Mitochondrial ribosomal protein of the large subunit, homolog of prokaryotic L29 ribosomal protein; located at the ribosomal tunnel exit.	yes
YMR072w	*ABF2* (1)	Mitochondrial DNA-binding protein involved in mitochondrial DNA replication and recombination, member of HMG1 DNA-binding protein family; activity may be regulated by protein kinase A phosphorylation.	yes
YMR155w	(1)	Unknown.	no

YMR173w	*DDR48* (1)	DNA damage-responsive protein, expression increases in response to heat-shock stress or treatments that produce DNA lesions; contains multiple repeats of amino acid sequence NNNDSYGS.	no
YMR192w	*GYL1* (1)	Putative GTPase activating protein (GAP) with role in exocytosis; stimulates Gyp5p GAP activity on Ypt1p, colocalizes with Gyp5p at sites of polarized growth; interacts with Gyp5p, Rvs161p, and Rvs167p.	no
YMR223w	*UBP8* (1)	Ubiquitin-specific protease, member of SAGA (Spt-Ada-Gcn5-Acetyltransferase) acetylation complex; required for SAGA-mediated deubiquitination of histone H2.	no
YPL183w-A	*RTC6* (1)	Protein involved in translation; mutants have defects in biogenesis of nuclear ribosomes; sequence similar to prokaryotic ribosomal protein L36, may be a mitochondrial ribosomal protein encoded in the nucleus.	yes
YPR100w	*MRPL51* (1)	Mitochondrial ribosomal protein of the large subunit.	yes

[a] Eight of the 17 gene deletions were confirmed independently to be responsible for resistance. Five deletion mutants were crossed to deletion strains of opposite mating type to generate homozygous diploids that exhibited the same phenotype (*GYL1*Δ,

406 *ABF2*Δ, *STP2*Δ, *NAM2*Δ, *BOI1*Δ). Two were transformed with wild-type alleles of the
407 deleted genes which restored sensitivity (*DDR48*, *CIR1*). One deletion mutant obtained
408 in a different strain background was also found to be resistant (*TRK1*Δ).
409 [b] Respiratory deficient as reported in references 6 or 19.
410
411
412
413
414
415 **Table 2.** Gene ontology (GO) analyses comparing the 17 genes deleted in the
416 AuTMAT-resistant mutants with the collection of 4,750 genes represented in the
417 deletion library from which the 17 were derived. The corrected *p* values indicate the
418 significance of the enrichment of genes with the associated terms. (Analysis was
419 performed 7 Aug 2011 (http://go.princeton.edu/cgi-bin/GOTermFinder/GOTermFinder).

GO Component Term	Frequency among 17 AuTMAT-resistant mutants	Library frequency (among 4750 genes)	Corrected *p* value	Genes annotated to term
Mitochondrial matrix	8 genes, 47.1%	174 genes, 3.7%	1.92×10^{-6}	YBR268w, YCR046c, YGR207c, YLR382c, YLR439w, YMR072w, YPL183w-A, YPR100w
Mitochondrial large ribosomal subunit	5 genes, 29.4%	41 genes, 0.9%	8.12×10^{-6}	YBR268w, YCR046c, YLR439w, YPL183w-A, YPR100w
Organelle lumen	9 genes, 52.9%	563 genes, 11.9%	0.00166	YBR268w, YCR046c, YGR207c, YLR382c, YLR439w, YMR072w, YMR223w, YPL183w-

				A, YPR100w

420

GO Process Term	Frequency among 17 AuTMAT-resistant mutants	Library frequency (among 4750 genes)	Corrected *p* value	Genes annotated to term
Mitochondrial organization	8 genes, 47.1%	238 genes, 5.0%	3.83×10^{-5}	YBR268w, YCR046c, YGR150c, YLR382c, YLR439w, YMR072w, YPL183w-A, YPR100w

421

422

423

424

GO Function Term	Frequency among 17 AuTMAT-resistant mutants	Library frequency (among 4750 genes)	Corrected *p* value	Genes annotated to term
Structural molecule activity	6 genes, 35.3%	254 genes, 5.3%	0.00248	YBR268w, YCR046c, YLR439w, YMR223w, YPL183w-A YPR100w
Structural constituent of ribosome	5 genes, 29.4%	177 genes, 3.7%	0.00437	YBR268w, YCR046c, YLR439w, YPL183w-A, YPR100w

425

426

427 **Table 3.** Resistant mutant cells killed as a function of 0.8 nm AuTMAT dose.

Deletion mutant	**Mutant cells killed as percentage of BY4742 cells killed at 10 ppm AuTMAT**	**Mutant cells killed as percentage of BY4742 cells killed at 100 ppm AuTMAT**
*MRPL51*Δ	**20.0**	**15.5**
*CUP2*Δ	**45.3**	**25.1**
*TRK1*Δ	**24.3**	**25.5**
*UBP8*Δ	**62.5**	**30.7**
*ABF2*Δ	>100	**30.7**
*DDR48*Δ	**48.2**	**37.3**
*STP2*Δ	**37.5**	**38.9**
*GYL1*Δ	**69.7**	**39.5**
*CCM1*Δ	**47.2**	**42.5**
*MRPL4*Δ	**66.4**	**43.1**
*CIR1*Δ	**52.4**	**51.2**
*MRPL37*Δ	**66.5**	**52.3**
*BOI2*Δ	90.3	**52.6**
*IMG1*Δ	93.5	**54.6**
*RTC6*Δ	86.9	**65.3**
*NAM2*Δ	**68.8**	**72.7**
*YMR155w*Δ	**50.7**	**86.0**

428 Data are mutant cells killed expressed as a percentage of BY4742 cells killed at the
429 same AuTMAT dose. Approximately 1-2 x 10^7 cells/ml were exposed to AuTMAT at the

indicated doses for 24 h in 100 µl aliquots. At the 10 and 100 ppm doses, 7.20 x 10^6 and 1.50 x 10^7 BY4742 cells/ml were killed. Data are means of three replicates for mutants and four to seven replicates for BY4742. Values in bold indicate that significantly fewer mutant than BY4742 cells were killed (p<0.05, Student's two-sided T-test).